PHILOSOPHICAL TRANSACTIONS A

royalsocietypublishing.org/journal/rsta

Research

Cite this article: Pan Y *et al*. 2021 Study of vibrational resonance in nonlinear signal processing. *Phil. Trans. R. Soc. A* **379**: 20200235. https://doi.org/10.1098/rsta.2020.0235

Accepted: 29 September 2020

One contribution of 11 to a theme issue 'Vibrational and stochastic resonance in driven nonlinear systems (part 1)'.

Subject Areas:
statistical physics, statistics

Keywords:
vibrational resonance, stochastic resonance, signal estimation, signal detection, sensor array

Author for correspondence:
Fabing Duan
e-mail: fabing.duan@gmail.com

Study of vibrational resonance in nonlinear signal processing

Yan Pan[1], Fabing Duan[2], François Chapeau-Blondeau[4], Liyan Xu[3] and Derek Abbott[5]

[1]College of Mathematics and Systems Science, Shandong University of Science and Technology, Qingdao 266590, People's Republic of China
[2]Institute of Complexity Science, and [3]School of Electronic Information, Qingdao University, Qingdao 266071, People's Republic of China
[4]Laboratoire Angevin de Recherche en Ingénierie des Systèmes (LARIS), Université d'Angers, 49000 Angers, France
[5]Centre for Biomedical Engineering and School of Electrical and Electronic Engineering, The University of Adelaide, Adelaide, Southern Australia 5005, Australia

YP, 0000-0001-6476-5457; FD, 0000-0003-1210-6825; DA, 0000-0002-0945-2674

Vibrational resonance (VR) intentionally applies high-frequency periodic vibrations to a nonlinear system, in order to obtain enhanced efficiency for a number of information processing tasks. Note that VR is analogous to stochastic resonance where enhanced processing is sought via purposeful addition of a random noise instead of deterministic high-frequency vibrations. Comparatively, due to its ease of implementation, VR provides a valuable approach for nonlinear signal processing, through detailed modalities that are still under investigation. In this paper, VR is investigated in arrays of nonlinear processing devices, where a range of high-frequency sinusoidal vibrations of the same amplitude at different frequencies are injected and shown capable of enhancing the efficiency for estimating unknown signal parameters or for detecting weak signals in noise. In addition, it is observed that high-frequency vibrations with differing frequencies can be considered, at the sampling times, as independent random variables. This property allows us here to develop a probabilistic analysis—much like in stochastic resonance—and to obtain a theoretical basis for the VR effect and its optimization for signal

THE ROYAL SOCIETY PUBLISHING

processing. These results provide additional insight for controlling the capabilities of VR for nonlinear signal processing.

This article is part of the theme issue 'Vibrational and stochastic resonance in driven nonlinear systems (part 1)'.

1. Introduction

Vibrational resonance (VR), firstly reported by Landa & McClintock [1], describes the resonant behaviour of the response of a bistable model to a low-frequency signal by optimizing the amplitude of a high-frequency periodic vibration. This interesting phenomenon, analogous to stochastic resonance [2–5], replaces artificially added noise with high-frequency vibrations, and has received considerable interest in nonlinear dynamics [1,6–16], neuroscience [17–22], engineering [23–27], information processing [28–30], etc. The mechanism of VR is elucidated in different systems with constant mass[1], and also extended to encompass systems with position-dependent mass (PDM) [11]. Compared to stochastic resonance, VR is easy to realize due to the ease of the implementation of intentionally injected high-frequency vibrations into nonlinear systems, especially in devices vibrations or jitter are already naturally present [31]. Motivated by this fact, we argue that the VR effect deserves to be extensively investigated in nonlinear devices within the framework of statistical signal processing.

In the field of statistical signal processing, in general the optimal signal processor is often too complex or intractable and we have to therefore employ suboptimal processors to deal with demanding signal processing tasks [32–34]. Moreover, for engineering applications such as remote sensing and environmental monitoring, a number of low-cost sensors with a few bits, e.g. quantizers, are often deployed over a sensing field to compose sensing networks. These scenarios motivate the investigation of VR for the performance improvement of nonlinear sensors by optimally tuning the amplitude of high-frequency vibrations. Here we will consider situations where an information bearing signal is transmitted and compressed by a number of nonlinear sensors, and then we inject a range of high-frequency periodic vibrations of the same amplitude at different frequencies into the sensor arrays for estimating unknown parameters or for detecting weak signals. We will show that, at the optimal vibration amplitude, the VR method can efficiently improve the estimation accuracy of unknown parameters and the detection probability of weak signals. In the view of the analogy between VR and stochastic resonance [1], we show that high-frequency vibrations with different frequencies can be regarded, at the sampling times, as mutually independent random variables with a common interval distribution. Based on this property, a probabilistic analysis is performed of the VR effect and its performance is analysed. Interestingly, numerical VR results agree well with the theoretical analyses based on stochastic resonance, which substantiates the analogy between VR and stochastic resonance in improving the information processing of nonlinear systems. These results reveal that intentional injection of high-frequency periodic vibrations into information-processing devices can be a beneficial option for nonlinear signal processing.

2. Vibrational resonance in location parameter estimation

We first consider a location parameter estimation problem according to the model

$$x_n = \theta + w_n,\ n = 1, 2, \ldots, N, \tag{2.1}$$

where θ is an unknown location parameter and the observation noise w_n are mutually independent with a common probability density function (PDF) f_w. For estimating the parameter

θ from the noisy data x_n, it is well known that maximum-likelihood principle is a useful approach to obtaining the practical estimator [32,33]

$$\hat{\theta} = \arg\min_{\theta} \sum_{n=1}^{N} \rho(x_n - \theta) \tag{2.2}$$

with the loss function $\rho(x) = -\log f_w$. Differentiating equation (2.2) with respect to θ yields

$$\sum_{n=1}^{N} \psi(x_n - \theta) = 0, \tag{2.3}$$

where $\hat{\theta}$ is the maximum-likelihood estimator for the function $\psi = -(\mathrm{d}f_w/\mathrm{d}w)/f_w \triangleq \psi_{\mathrm{MLE}}$ [32,33].

However, in practice, the PDF f_w may be incompletely known or the observation data may be corrupted by outliers, which greatly degrades efficiency of the maximum-likelihood estimator [33]. Therefore, we often employ some robust estimators that are insensitive to outliers. For instance, we here consider the bisquare estimator with the redescending function

$$\psi(x) = x\left[1 - \left(\frac{x}{\gamma}\right)^2\right]^2, \tag{2.4}$$

for $|x| \le \gamma$ and otherwise zero, and the adjustable parameter γ. There are also other robust estimator related to the function ψ (not shown here) [33]. In order to reach a better trade-off between robustness and efficiency, we demonstrated with the function of equation (2.4) the improvement of the asymptotic efficiency and the reduction of the maximum bias by adding noise to robust estimators [35]. As an alternative of noise-enhanced mechanism, VR is also another interesting approach for estimating the location parameter in the observation model of equation (2.1). Here, we inject high-frequency sinusoidal vibrations $\eta_{mn} = A_\eta \sin(2\pi f_m n)$ of the same amplitude A_η but with different frequencies f_m to the original observations x_n, resulting in updated observations

$$y_{mn} = x_n + \eta_{mn} = \theta + z_{mn},\ n = 1, 2, \ldots, N, \tag{2.5}$$

where $z_{mn} = w_n + \eta_{mn}$ for $m = 1, 2, \ldots, M$ ($M \ge 1$). Here, it is noted that the frequency f_m is regarded as a uniform variable with its lower bound much larger than the sampling frequency $1/T$ with $T = 1$. Then, we have M estimators $\hat{\theta}_m$ defined as M roots of equation (2.3), i.e. $\sum_{n=1}^{N} \psi(y_{mn} - \hat{\theta}_m) = 0$. Collecting these estimators $\hat{\theta}_m$, we can design a VR-based location estimator as

$$\hat{\theta} = \frac{1}{M} \sum_{m=1}^{M} \hat{\theta}_m. \tag{2.6}$$

For the implementation of the designed estimator in equation (2.6), we can adopt the iterative reweighting method to obtain the numerical estimation of a location parameter [33]. Denoting

$$\Psi(x) = \begin{cases} \frac{\psi(x)}{x}, & x \neq 0, \\ \psi'(x), & x = 0, \end{cases} \tag{2.7}$$

then equation (2.3) can be rewritten as $\sum_{n=1}^{N} \Psi(x_n - \hat{\theta})(x_n - \hat{\theta}) = 0$. In line with this, each estimator $\hat{\theta}_m$ in equation (2.6) can be numerically computed as

$$\hat{\theta}_m(k+1) = \frac{\sum_{n=1}^{N} \Psi_{mn}(k)\, y_{mn}}{\sum_{n=1}^{N} \Psi_{mn}(k)} \tag{2.8}$$

with the weight function $\Psi_{mn}(k) = \Psi[y_{mn} - \hat{\theta}_m(k)]$ at the kth iteration for $k = 0, 1, 2, \ldots$. Here, the initial value $\hat{\theta}_m(0)$ is taken as the median of the updated observations y_{mn} in equation (2.5). When $|\hat{\theta}_m(k^* + 1) - \hat{\theta}_m(k^*)| < \zeta$ for a small tolerance ζ, the numerical estimator $\hat{\theta}_m(k^* + 1)$ is assumed to be the targeted estimator $\hat{\theta}_m$. A sufficiently large number of Monte Carlo trials of $\hat{\theta}_m$ is carried out by the above iterative reweighting method, and the variance $\mathrm{var}(\hat{\theta})$ of $\hat{\theta}$ in equation (2.6) can be numerically evaluated for a given size M. Compared with the variance $\mathrm{var}(\hat{\theta}_{\mathrm{MLE}}) = [NJ(f_w)]^{-1}$

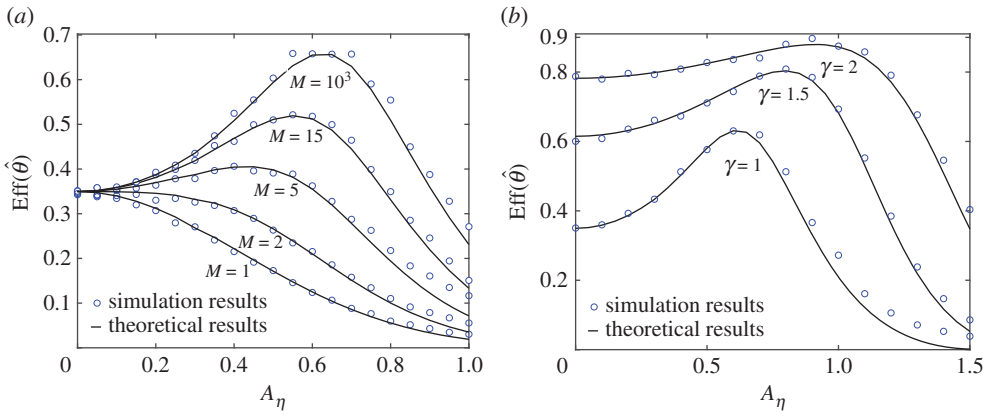

Figure 1. Asymptotic efficiency Eff($\hat{\theta}$) in equation (2.9) of the VR-based estimator in equation (2.6) as a function of the amplitude A_η of high-frequency sinusoidal vibrations η_{mn} for Cauchy noise. (*a*) Bisquare estimators $\hat{\theta}_m$ are with the parameter $\gamma = 1$ and the collective estimator number $M = 1, 2, 5, 15, 10^3$ from the bottom up. (*b*) The estimator number $M = 10^2$, and the parameter $\gamma = 1, 1.5$ and 2. Here, the observation size $N = 10^3$, the number of simulation trails is 10^4 and the tolerance constant $\zeta = 10^{-6}$. For each trail, the frequencies of high-frequency sinusoidal vibrations η_{mn} are uniformly taken from the interval $[10^2, 2 \times 10^3]$. (Online version in colour.)

achieved by the maximum-likelihood estimator denoted by ψ_{MLE} [33], the asymptotic large-N efficiency of the designed estimator $\hat{\theta}$ in equation (2.6) is defined as

$$\mathrm{Eff}(\hat{\theta}) = \frac{\mathrm{var}(\hat{\theta}_{\mathrm{MLE}})}{\mathrm{var}(\hat{\theta})}, \tag{2.9}$$

where $J(f_w) = E_w[(f_w'/f_w)^2]$ is the Fisher information of PDF f_w and the expectation operator $E_w(\cdot) = \int \cdot f_w(x)dx$ [35].

For example, we here consider a typical heavy-tailed distribution model of the Cauchy background noise w_n with PDF $f_w(x) = [\pi(1 + x^2)]^{-1}$. For the VR-based location estimator $\hat{\theta}$ in equation (2.6) composed of M bisquare estimators $\hat{\theta}_m$ with the parameter $\gamma = 1$, we plot the numerical asymptotic efficiency Eff($\hat{\theta}$) of equation (2.9) (○) as a function of the amplitude A_η of high-frequency sinusoidal vibrations in figure 1*a*. It is seen that, for a single estimator with $M = 1$, the asymptotic efficiency Eff($\hat{\theta}$) of equation (2.9) monotonically decreases with the increase of A_η. However, due to the collective role of estimator number $M > 1$ illustrated in figure 1*a*, the high-frequency sinusoidal vibrations η_{mn} can maximize the asymptotic efficiency Eff($\hat{\theta}$) at an optimal amplitude A_η^{opt}, which is the VR effect in the location parameter estimation. For instance, for the collective number $M = 10^3$ and without the help of high-frequency sinusoidal vibrations ($A_\eta = 0$), the asymptotic efficiencies Eff($\hat{\theta}$) = 0.3450. At the optimal amplitude $A_\eta^{\mathrm{opt}} = 0.65$, Eff($\hat{\theta}$) can be achieved its maximum value 0.6582, as shown in figure 1*a*. Moreover, for a fixed estimator number $M = 10^2$, the asymptotic efficiencies Eff($\hat{\theta}$) in equation (2.9) of the VR-based estimator in equation (2.6), as indicated in figure 1*b*, can be also optimized by the amplitude A_η for different parameter values of γ. It is noted in figure 1*b* that, for a wide range of estimator parameter γ, the VR effect survives and the asymptotic efficiency Eff($\hat{\theta}$) in equation (2.9) of the designed estimator benefits from the injection of high-frequency sinusoidal vibrations.

In addition, since there is a clear analogy between stochastic resonance and VR [1], then the random variable (noise) with the PDF

$$f_\eta(x) = \frac{1}{\pi\sqrt{A_\eta^2 - x^2}}, \ -A_\eta < x < A_\eta \tag{2.10}$$

can be used to describe the distribution of a sinusoidal vibration with amplitude A_η. Here, we argue that different frequencies f_m of high-frequency sinusoidal vibrations η_{mn} correspond to the different samples of this variable. This mapping of high-frequency sinusoidal vibrations into noise samples allows us to develop a probabilistic theoretical analysis of VR within the framework of stochastic resonance. In our previous work [35], applying the first-order Taylor expansion of ψ for each estimator $\hat{\theta}_m$ around the true value of θ, we derive the asymptotic variance of the designed estimator in equation (2.6) as

$$\mathrm{var}_a(\hat{\theta}) = \frac{1}{N}\frac{E_z[\psi^2(z)] + (M-1)E_w\{E_\eta^2[\psi(w+\eta)]\}}{ME_z^2[\psi'(z)]}, \tag{2.11}$$

where the convolved PDF $f_z(z) = \int f_w(z-\eta)f_\eta(\eta)\,\mathrm{d}\eta$ for the composite variable z_{mn}, the expectations $E_z(\cdot) = \int \cdot f_z(x)\,\mathrm{d}x$ and $E_\eta(\cdot) = \int \cdot f_\eta(x)\,\mathrm{d}x$. Substituting equation (2.10) and equation (2.11) into equation (2.9), we can theoretically calculate the asymptotic efficiency $\mathrm{Eff}(\hat{\theta})$ in equation (2.9) of the designed estimator in equation (2.6) within the theoretical framework of stochastic resonance [35]. It is clearly seen by the comparison of figure 1 that the theoretical results (solid lines) calculated by equation (2.11) agree well with the numerical simulation results (○) obtained by the experiments with the injection of high-frequency sinusoidal vibrations into estimators. This evidence not only demonstrates the similarity between the two phenomena of VR and stochastic resonance stated in [1], but also provides a theoretical approach to investigate the VR effect in parameter estimation problems.

3. Vibrational resonance in Bayesian estimation

In §2, the location θ is assumed to be a deterministic but unknown parameter. However, we cannot incorporate our prior knowledge about the parameter θ into the designed estimator [32]. Instead, we need to assume that θ is a random variable with a prior PDF f_θ and design an estimator based on Bayes' theorem [32]. In this section, we will study the potential application of VR in Bayesian estimators for improving the estimation accuracy of random parameter estimation.

Consider a random parameter estimation model with the observation

$$x = \theta + w \tag{3.1}$$

where the random parameter θ has the prior PDF f_θ, and the background white noise w, independent of θ, has the PDF f_w. Then, the observation x accords with the convolved PDF $f_x(x) = \int f_w(x-\theta)f_\theta(\theta)\mathrm{d}\theta$. For the quadratic cost function, the optimal estimator is the mean of posterior PDF given by

$$\hat{\theta}_{\mathrm{mmse}}(x) = \frac{\int \theta f_w(x-\theta)f_\theta(\theta)\,\mathrm{d}\theta}{\int f_w(x-\theta)f_\theta(\theta)\,\mathrm{d}\theta}, \tag{3.2}$$

which is regarded as the minimum mean square error (MMSE) estimator [32]. However, the MMSE estimator $\hat{\theta}_{\mathrm{mmse}}$ is often difficult to be solved in a close form. Thus, in practice, some feasible nonlinear Bayesian estimators with explicit forms are usually employed. In the context of stochastic resonance, Uhlich [36] proposed a novel noise-enhanced estimator by averaging estimates from the same observation added by artificial noise components, and discussed its superiority over the original estimator. We further investigate the benefits of intentionally adding noise to the estimator and present a combined Bayesian estimator with a set of optimum weighting coefficients [37]. Inspired by the work [36,37] and the analogy between VR and stochastic resonance, we add the high-frequency sinusoidal vibrations to M suboptimal Bayesian estimators $\hat{\theta}_m$ and establish a VR-based Bayesian estimator as

$$\hat{\theta}(x) = \frac{1}{M}\sum_{m=1}^{M}\hat{\theta}_m[x + A_\eta \sin(2\pi f_m n_0)], \tag{3.3}$$

where the time n_0 is arbitrary and the frequency f_m is a random variable with a uniform distribution.

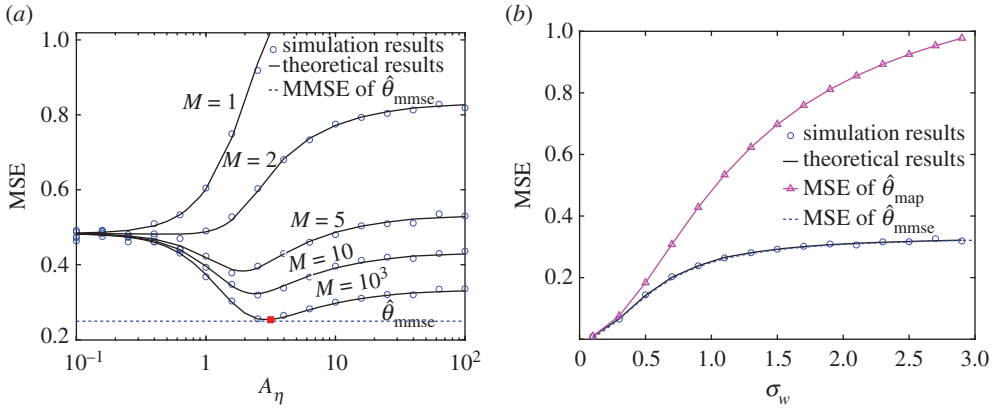

Figure 2. (*a*) Numerical and theoretical results of MSEs of the designed Bayesian estimator $\hat{\theta}$ in equation (3.4) composed of M numbers of MAP estimators $\hat{\theta}_{\text{map}}$ of equation (3.5) versus the vibration amplitude A_η. For comparison, the MMSE estimator $\hat{\theta}_{\text{mmse}}$ is also plotted. Here, the background noise level $\sigma_w = 1$ and the interval bound $a = 2$ for the parameter θ. (*b*) For a fixed number $M = 10^3$ and at the optimal vibration amplitudes A_η^{opt}, the MSEs of the designed Bayesian estimator $\hat{\theta}$ versus the background noise level σ_w. For comparison, MSEs of the MAP estimator $\hat{\theta}_{\text{map}}$ and the MMSE estimator $\hat{\theta}_{\text{mmse}}$ versus the background noise level σ_w are also plotted. (Online version in colour.)

In the numerical experiments, for a sufficiently large number K of random values of θ_k distributed by the prior PDF f_θ, K Monte Carlo trails of the designed estimator in equation (3.3) are carried out and the numerical MSE can be computed as

$$\text{MSE}(\hat{\theta}) = \frac{1}{K}\sum_{k=1}^{K}[\hat{\theta}(x_k) - \theta_k]^2 = \frac{1}{K}\sum_{k=1}^{K}\left\{\frac{1}{M}\sum_{m=1}^{M}\hat{\theta}_m\left[x_k + A_\eta \sin(2\pi f_m n_0)\right] - \theta_k\right\}^2. \tag{3.4}$$

For instance, consider a uniformly distributed parameter θ buried in the Gaussian white noise w [32,36]. The prior PDF of θ is $f_\theta(x) = 1/a$ for $0 \le x \le a$ and otherwise zero, and w has its PDF $f_w(x) = \exp(-x^2/2\sigma_w^2)/\sqrt{2\pi\sigma_w^2}$ with zero-mean and variance σ_w^2. Under this situation, the maximum *a posteriori* (MAP) estimator is given by

$$\hat{\theta}_{\text{map}}(x) = \begin{cases} 0, & x < 0, \\ x, & 0 \le x \le a, \\ a, & x > a, \end{cases} \tag{3.5}$$

which has the MSE 0.4832 for the interval bound $a = 2$ and the background noise level $\sigma_w = 1$. Then, we collect M MAP estimators $\hat{\theta}_{\text{map}}$ driven by M high-frequency sinusoidal vibrations and plot the numerical MSE of the designed Bayesian estimator in equation (3.4) as a function of the vibration amplitude A_η in figure 2*a*. It is seen that, upon increasing the vibration amplitude A_η and the number $M > 2$, the numerical MSE (○) of the designed Bayesian estimator in equation (3.4) is reduced to a minimum value at an optimal amplitude A_η^{opt}. In addition, when $M = 10^3$, the VR effect is more effective and can reduce the initial MSE value 0.4832 at $A_\eta = 0$ to the minimum of 0.2531 (square) at the optimal amplitude $A_\eta^{\text{opt}} = 3.162$. It is also noted that this minimum value of 0.2531 is closely near to the MSE of 0.2492 (dashed line) achieved by the MMSE estimator $\hat{\theta}_{\text{mmse}}$ [32,36,37]. It is emphasized that, upon increasing the number $M > 10^3$ and at the optimal vibration amplitude A_η, the MSE of the designed Bayesian estimator $\hat{\theta}$ in equation (3.4) can gradually approach the MMSE 0.2492, but the computation in Monte Carlo simulation is too heavy.

Next, by the probabilistic modelling based on the random variable with the PDF in equation (2.10), we theoretically calculate the MSE of the designed Bayesian estimator in equation (3.4) composed of M estimators $\hat{\theta}_{\text{map}}$ as

$$\begin{aligned}\text{MSE}(\hat{\theta}) &= E_{x,\eta}[(\hat{\theta}-\theta)^2] \\ &= E_\theta(\theta^2) - \frac{2}{M}\sum_{m=1}^{M} E_{x,\eta}[\theta\hat{\theta}_{\text{map}}(x+\eta_m)] \\ &\quad + \frac{1}{M^2}\left\{\sum_{m=1}^{M} E_{x,\eta}[\hat{\theta}^2_{\text{map}}(x+\eta_m)] + \sum_{l=1}^{M}\sum_{k=1}^{M} E_{x,\eta}[\hat{\theta}_{\text{map}}(x+\eta_l)\hat{\theta}_{\text{map}}(x+\eta_k)]\right\}(l\neq k) \\ &= E(\theta^2) - 2E_x\{\theta E_\eta[\hat{\theta}_{\text{map}}(x+\eta)]\} + \frac{1}{M}E_x\{E_\eta[\hat{\theta}^2_{\text{map}}(x+\eta)]\} \\ &\quad + \frac{M-1}{M}E_x\{E^2_\eta[\hat{\theta}_{\text{map}}(x+\eta)]\},\end{aligned} \tag{3.6}$$

where $E_{x,\eta}$ denotes the expectation with respect to the joint PDF of variable x and η and $E_\theta(\cdot)$ denotes the expectation with respect to the PDF of variable θ. Under the assumption of the PDF f_η in equation (2.10), it is noted that $E_\eta[\hat{\theta}_{\text{map}}(x+\eta_l)] = E_\eta[\hat{\theta}_{\text{map}}(x+\eta_k)]$ for $l\neq k$ and $l,k=1,2,\ldots,M$. Using equation (3.6) derived within the framework of stochastic resonance, the theoretical MSEs of the designed Bayesian estimator in equation (3.4) are also shown in figure 2*a* as a function of the distribution parameter A_η in equation (2.10). It is clearly shown that the theoretical results (solid lines) obtained by equation (3.6) accord with the simulation results (○) with high-frequency sinusoidal vibrations. Furthermore, we illustrate the minimum MSE of the designed Bayesian estimator in equation (3.4) theoretically and numerically for different background noise level σ_w in figure 2*b*. It is noted that, without the help of vibrations ($A_\eta = 0$), the MSE (△) of MAP estimator $\hat{\theta}_{\text{map}}$ is much higher than the MSE (dashed line) achieved by the MMSE estimator $\hat{\theta}_{\text{mmse}}$. However, due to the positive role of high-frequency sinusoidal vibrations with optimal amplitudes, both numerical (○) and theoretical (black solid line) MSEs of the designed Bayesian estimator in equation (3.4) are rather comparable with the MSE (dashed line) achieved by the MMSE estimator $\hat{\theta}_{\text{mmse}}$.

4. Vibrational resonance in weak-signal detection

The VR effect can be also exploited to detect weak signals in the presence of strong background noise. Consider a binary hypothesis detection problem

$$\left.\begin{aligned} &H_0 : x_n = \theta s_n + w_n \\ \text{and}\quad &H_1 : x_n = w_n,\ n = 1,2,\ldots,N,\end{aligned}\right\} \tag{4.1}$$

where s_n represent the known signalling waveforms with unknown amplitude $\theta > 0$ and w_n are mutually independent and identically distributed (i.i.d.) white noise components. For detecting the weak signals with $\theta \to 0$, the locally optimum detector is based on the knowledge of the PDF f_w [30,32,34], and it may not be easily accessible or implementable for many practical problems of interest. Then, the generalized correlation detector is often employed to select H_0 or H_1 on the observations x_n [34]. Inspired by the VR mechanism, we construct a generalized correlation detector

$$T_{\text{HF}} = \sum_{n=1}^{N}\left[\frac{1}{M}\sum_{m=1}^{M} g(x_n+\eta_{mn})\right]s_n \underset{H_0}{\overset{H_1}{\gtrless}} \gamma \tag{4.2}$$

by injecting M high-frequency vibrations $\eta_{mn} = A_\eta \sin(2\pi f_m n)$ plus x_n into the transfer function g, where γ is the decision threshold [30]. Under the assumption of zero expectation of the

memoryless transfer function g, i.e. $\mathrm{E}[g(x)]=0$, and for a given false alarm probability P_{FA}, the detection probability P_{D} can be calculated as [30,32,34]

$$P_{\mathrm{D}}=Q[Q^{-1}(P_{\mathrm{FA}})-\sqrt{R_{\mathrm{out}}}], \tag{4.3}$$

where $Q^{-1}(x)$ is the inverse function of $Q(x)=\int_x^\infty \exp(-t^2/2)/\sqrt{2\pi}\,\mathrm{d}t$. Here, the output signal-to-noise ratio (SNR) of R_{out} is given by

$$R_{\mathrm{out}}=\frac{[E(T_{\mathrm{HF}}|H_1)-E(T_{\mathrm{HF}}|H_0)]^2}{\mathrm{var}(T_{\mathrm{HF}}|H_0)} \tag{4.4}$$

with the variance $\mathrm{var}(T_{\mathrm{HF}}|H_0)\approx\mathrm{var}(T_{\mathrm{HF}}|H_1)$ and $E[T_{\mathrm{HF}}|H_i]$ and $\mathrm{var}(T_{\mathrm{HF}}|H_i)$ represent the expectation and the variance under the hypothesis H_i for $i=0,1$, respectively.

For instance, consider the weak signal $s_n=\theta\sin(2\pi f_s n)$ with $\theta=0.0711$ and $f_s=10^{-3}$ and the background Laplacian noise w has its PDF $f_w(x)=\exp(-\sqrt{2}|x/\sigma_w|)/(\sqrt{2}\sigma_w)$ and variance $\sigma_w^2=0.8$. Then, the input SNR $R_{\mathrm{in}}=10\log_{10}(\theta^2/2\sigma_w^2)=-25\,\mathrm{dB}$. The transfer function in equation (4.2) is given by

$$g(x)=\begin{cases}-1, & x\leqslant-\Theta,\\ 0, & -\Theta<x\leqslant\Theta,\\ 1, & x>\Theta,\end{cases} \tag{4.5}$$

with the threshold $\Theta\geq 0$, which is easily implementable in practice and tractable analytically. Here, it is noted that the frequencies f_m of the vibrations $\eta_{mn}=A_\eta\sin(2\pi f_m n)$ are much higher than the input signal frequency f_s, i.e. $f_m\gg f_s$. To set the decision threshold and obtain the numerical values of the detection probability P_{D} from equations (4.3) and (4.4), the calculation analysis in [30] is very complex. Instead, we perform probabilistic modelling employing the PDF defined in equation (2.10) to determine the decision threshold γ and theoretically analyse the detection probabilities P_D in equation (4.3).

For a sufficiently large observed size N, the statistic T_{HF} in equation (4.2) will be asymptotically Gaussian. Therefore, under the null hypothesis H_0 and for the composite noise $z=w+\eta$, the mean $\mathrm{E}_z[T_{\mathrm{HF}}|H_0]=E_z[g(z)]\sum_{n=1}^N s_n=0$ and the variance

$$\begin{aligned}\mathrm{var}[T_{\mathrm{HF}}|H_0]&=E_z[T_{\mathrm{HF}}^2|H_0]-E_z^2[T_{\mathrm{HF}}|H_0]\\&=\sum_{n=1}^N s_n^2\Big\{\frac{1}{M}E_z[g^2(z)]+\frac{(M-1)}{M}E_w\big\{E_\eta^2[g(w+\eta)]\big\}\Big\}.\end{aligned} \tag{4.6}$$

Under the hypothesis H_1 and as the weak signal strength $\theta\to 0$, the mean has the asymptotic form

$$\begin{aligned}E_z[T_{\mathrm{HF}}|H_1]&=E_z\left[\sum_{n=1}^N\frac{1}{M}\sum_{m=1}^M g(\theta s_n+z_{mn})s_n\right]\\&\approx E_z\left\{\sum_{n=1}^N[g(z)+\theta s_n g'(z)]s_n\right\}\\&=\theta\sum_{n=1}^N s_n^2E_z[g'(z)],\end{aligned} \tag{4.7}$$

and variance $\mathrm{var}[T_{\mathrm{GC}}|H_1]\approx\mathrm{var}[T_{\mathrm{GC}}|H_0]$. Then, substituting $E[T_{\mathrm{HF}}|H_i]$ and $\mathrm{var}(T_{\mathrm{HF}}|H_i)$ into equation (4.4), we can evaluate the detection probabilities P_{D} (solid lines) in equation (4.3) theoretically, as shown in figure 3*a*. It is seen that, for a fixed false alarm probability $P_{\mathrm{FA}}=10^{-2}$ and a given number M, the detection probabilities P_{D} in equation (4.3) can be maximized at an optimal amplitude A_η^{opt}. Furthermore, as the number M increases, we plot the maximum P_D by optimizing the vibration amplitude A_η numerically (○) and theoretically (solid lines) in figure 3*b*. It is indicated in figure 3*b* that, even for a moderate number $M=200$, the initial $P_{\mathrm{D}}=0.45$ can be improved to the maximum $P_{\mathrm{D}}=0.9232$ via the VR method, which approaches to the detection

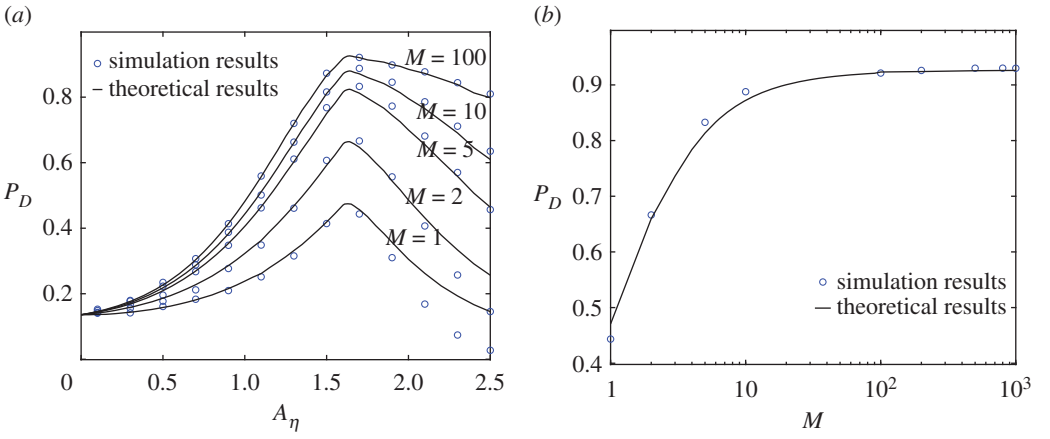

Figure 3. (*a*) Detection probability P_D of equation (4.3) versus the interference amplitude A_η, and (*b*) Maximum P_D obtained by the optimal amplitude A_η versus the number M. In numerical experiments, the values of the detection probability (circles) are achieved by the Monte–Carlo simulation method [32]. Using equation (4.6), the decision threshold $\gamma = \sqrt{\mathrm{var}(T_{HF}|H_0)}Q^{-1}(P_{FA})$ can be obtained for a given false alarm probability P_{FA}. Then, generating N independent random variables $x_n = w_n$ or $x_n = s_n + w_n$, we inject M high-frequency vibrations η_{nm} with the same amplitude A_η at different frequencies into each observation x_n. We numerically compute the statistic T_{HF} in equation (4.2) and compare it with the threshold γ for a number of realizations of 10^5, and then the detection probability $\hat{P}_D$ is obtained as the ratio of the number of $T_{HF} > \gamma$ over the total realizations. Here, the threshold $\Theta = 1.6$, the observation length $N = 3000$, the false alarm probability $P_{FA} = 0.01$, and the input SNR $R_{in} = -25$ dB for the signal strength $\theta = 0.0711$. (Online version in colour.)

probability $P_D = 0.97$ achieved by the locally optimum detector [32,34]. Numerical simulations (○) and theoretical analyses (solid line) of VR-based detector in equation (4.2), as indicated in figure 3, are valuable in detecting weak signals. For other types of noise w, similar results are also obtained and not shown here for simplicity.

5. Conclusion

In this paper, we investigated the VR effect for the improvement of signal processors for estimating unknown parameters and detecting weak signals. For a number of nonlinear sensors, we inject a spread of high-frequency sinusoidal electrical signals into the sensors and collect their responses for nonlinear signal processing. It is noted that the sinusoidal amplitudes are identical, but their frequencies are different. Upon increasing the number of sensors and the sinusoidal amplitude, the VR effect becomes more and more effective in improving the estimation accuracy and the signal detectability. Since the VR effect can be perceived as a form of stochastic resonance, then we consider the sinusoid amplitude as a random variable (noise) with an interval distribution. This mapping of the sinusoidal vibration amplitude to a random variable brings convenience to theoretically calculate the resonance behaviour of VR within the framework of stochastic resonance. Both numerical and theoretical results demonstrate that the VR effect is a potential method for some demanding nonlinear signal processing tasks in practice.

For enhancing the performance of estimators and detectors, the explicit or approximate forms of optimal added noise have been derived or approximately solved [35–37]. It is proven that, with the help of optimal noise, the stochastic resonance-based estimator or detector achieves a rather comparable performance to the optimal processor [35–37]. Beyond the optimization of the amplitude of vibrations, non-sinusoidal high-frequency vibrations, such as high-frequency square and sawtooth vibrations, could be optimized to investigate the possibility of a still enhanced performance of the VR-based processors. This is of interest and remains an open question for future studies. In addition, for a variety of background noise types, we need to optimize the

vibration amplitude to enhance the performance of processors. Thus, for exploiting the VR effect in practical signal processing tasks, an adaptive algorithm of finding the optimal vibration amplitude, frequency or vibration waveforms deserves to be further studied.

Data accessibility. Data are provided in the electronic supplementary material.

Authors' contributions. Y.P. and F.D. carried out the experiments. F.D. and L.X. performed the data analysis. Y.P., F.D., F.C.B. and D.A. conceived of and designed the study, and drafted the manuscript. All authors read and approved the manuscript.

Competing interests. We declare we have no competing interests.

Funding. This work was funded by the National Natural Science Foundation of China (grant nos. 62001271 and 61573202).

Acknowledgements. We sincerely thank the editors and the anonymous reviewers for their suggestions and comments.

References

1. Landa PS, McClintock PVE. 1993 Vibrational resonance. *J. Phys. A: Math. Gen.* **33**, L433–L438. (doi:10.1088/0305-4470/33/45/103)
2. Benzi R, Sutera A, Vulpiani A. 1981 The mechanism of stochastic resonance. *J. Phys. A: Math. Gen.* **14**, L453–L457. (doi:10.1088/0305-4470/14/11/006)
3. McClintock PVE. 1999 Unsolved problems of noise. *Nature* **401**, 23–25. (doi:10.1038/43331)
4. Kwasniok F. 2014 Enhanced regime predictability in atmospheric low-order models due to stochastic forcing. *Phil. Trans. R. Soc. A* **372**, 20130286. (doi:10.1098/rsta.2013.0286)
5. Bashkirtseva I, Pankratov A, Slepukhina E, Tsvetkov I. 2020 Constructive role of noise and diffusion in an excitable slow-fast population system. *Phil. Trans. R. Soc. A* **378**, 20190253. (doi:10.1098/rsta.2019.0253)
6. Vincent UE, Roy-Layinde TO, Popoola OO, Adesina PO, McClintock PVE. 2018 Vibrational resonance in an oscillator with an asymmetrical deformable potential. *Phys. Rev. E* **98**, 062203. (doi:10.1103/PhysRevE.98.062203)
7. Chizhevsky VN, Giacomelli G. 2004 Experimental and theoretical study of the noise-induced gain degradation in vibrational resonance. *Phys. Rev. E* **70**, 062101. (doi:10.1103/PhysRevE.70.062101)
8. Ghosh S, Ray DS. 2013 Nonlinear vibrational resonance. *Phys. Rev. E* **88**, 042904. (doi:10.1016/10.1103/PhysRevE.88.042904)
9. Sarkar P, Paul S, Ray DS. 2019 Controlling subharmonic generation by vibrational and stochastic resonance in a bistable system. *J. Stat. Mech. Theory Exp.* **2019**, 063211. (doi:10.1088/1742-5468/ab2532)
10. Gandhimathi VM, Rajasekar S, Kurths J. 2006 Vibrational and stochastic resonances in two coupled overdamped anharmonic oscillators. *Phys. Lett. A* **360**, 279. (doi:10.1016/j.physleta.2006.08.051)
11. Roy-Layinde TO, Vincent UE, Abolade SA, Popoola OO, Laoye JA, McClintock PVE. 2021 Vibrational resonances in driven oscillators with position-dependent mass. *Phil. Trans. R. Soc. A* **379**, 20200227. (doi:10.1098/rsta.2020.0227)
12. Kremer E. 2021 The effect of high-frequency stochastic actions on the low-frequency behaviour of dynamic systems. *Phil. Trans. R. Soc. A* **379**, 20200242. (doi:10.1098/rsta.2020.0242)
13. Paul S, Shankar Ray D. 2021 Vibrational resonance in a driven two-level quantum system, linear and nonlinear response. *Phil. Trans. R. Soc. A* **379**, 20200231. (doi:10.1098/rsta.2020.0231)
14. Sorokin V, Demidov I. 2021 On representing noise by deterministic excitations for interpreting the stochastic resonance phenomenon. *Phil. Trans. R. Soc. A* **379**, 20200229. (doi:10.1098/rsta.2020.0229)
15. Wadop Ngouongo YJ, Djolieu Funaye M, Djuidjé Kenmoé G, Kofané TC. 2021 Stochastic resonance in deformable potential with time-delayed feedback. *Phil. Trans. R. Soc. A* **379**, 20200234. (doi:10.1098/rsta.2020.0234)
16. Coccolo M, Cantisán J, Seoane JM, Rajasekar S, Sanjuán MAF. 2021 Delay-induced resonance suppresses damping-induced unpredictability. *Phil. Trans. R. Soc. A* **379**, 20200232. (doi:10.1098/rsta.2020.0232)

17. Bordet M, Morfu S, Marquié P. 2015 Ghost responses of the FitzHugh-Nagumo system induced by colored noise. *Chaos, Solitons Fractals* **78**, 205–214. (doi:10.1016/j.chaos.2015.07.032)
18. Ullner E, Zaikin A, García-Ojalvo J, Bascones R, Kurths J. 2003 Vibrational resonance and vibrational propagation in excitable systems. *Phys. Lett. A* **312**, 348–354. (doi:10.1016/S0375-9601(03)00681-9)
19. Hu DL, Yang JH, Liu XB. 2014 Vibrational resonance in the FitzHugh–Nagumo system with time-varying delay feedback. *Comput. Biol. Med.* **45**, 80–86. (doi:10.1016/j.compbiomed.2013.11.022)
20. Yang JH, Sanjuán MAF, Liu HG. 2015 Vibrational subharmonic and superharmonic resonances. *Commun. Nonlinear Sci. Numer. Simul.* **30**, 362–372. (doi:10.1016/j.cnsns.2015.07.002)
21. Uzuntarla M, Yilmaz E, Wagemakers A, Ozer M. 2015 Vibrational resonance in a heterogeneous scale free network of neurons. *Commun. Nonlinear Sci. Numer. Simul.* **22**, 367–374. (doi:10.1016/j.cnsns.2014.08.040)
22. Agaoglu SN, Calim A, Hoevel P, Ozer M, Uzuntarla M. 2019 Vibrational resonance in a scale-free network with different coupling schemes. *Neurocomputing* **325**, 59–66. (doi:10.1016/j.neucom.2018.09.070)
23. Chizhevsky VN, Giacomelli G. 2005 Improvement of signal-to-noise ratio in a bistable optical system: Comparison between virational and stochastic resonance. *Phys. Rev. A* **71**, 011801. (doi:10.1103/PhysRevA.71.011801)
24. Venkatesh PR, Venkatesan A. 2016 Vibrational resonance and implementation of dynamic logic gate in a piecewise-linear Murali Lakshmanan Chua circuit. *Commun. Nonlinear Sci. Numer. Simul.* **39**, 271. (doi:10.1016/j.cnsns.2016.03.009)
25. Chizhevsky VN. 2021 Amplification of optical signals in a bistable vertical-cavity surface-emitting laser by vibrational resonance. *Phil. Trans. R. Soc. A* **379**, 20200241. (doi:10.1098/rsta.2020.0241)
26. Murali K, Rajasekar S, Manaoj Aravind V, Kohar V, Ditto WL, Sinha S. 2021 Construction of logic gates exploiting resonance phenomena in nonlinear systems. *Phil. Trans. R. Soc. A* **379**, 20200238. (doi:10.1098/rsta.2020.0238)
27. Yang C, Yang J, Zhou D, Zhang S, Litak G. 2021 Adaptive stochastic resonance in bistable system driven by noisy NLFM signal: phenomenon and application. *Phil. Trans. R. Soc. A* **379**, 20200239. (doi:10.1098/rsta.2020.0239)
28. Morfu S, Usama BI, Marquié P. 2019 Perception enhancement of subthreshold noisy image with vibrational resonance. *Electron. Lett.* **55**, 650–652. (doi:10.1049/el.2018.8059)
29. Duan F, Chapeau-Blondeau F, Abbott D. 2014 Double-maximum enhancement of signal-to-noise ratio gain via stochastic resonance and vibrational resonance. *Phys. Rev. E* **90**, 022134. (doi:10.1103/PhysRevE.90.022134)
30. Ren Y, Pan Y, Duan F, Chapeau-Blondeau F. 2017 Exploiting vibrational resonance in weak-signal detection. *Phys. Rev. E* **96**, 022141. (doi:10.1103/PhysRevE.96.022141)
31. Stephens R. 2004 Analyzing jitter at high data rates. *IEEE Commun. Mag.* **42**, S6–S10. (doi:10.1109/MCOM.2003.1267095)
32. Kay S. 1998 *Fundamentals of statistical signal Processing–Detection theory*. Englewood Cliffs, NJ: Prentice-Hall.
33. Maronna R, Martin D, Yohai V. 2006 *Robust statistics: theory and methods*. New York, NY: Wiley.
34. Kassam SA. 1988 *Signal detection in non-Gaussian noise*. New York, NY: Springer.
35. Pan Y, Duan F, Chapeau-Blondeau F, Abbott D. 2018 Noise enhancement in robust estimation of location. *IEEE Trans. Signal Process.* **66**, 1953–1966. (doi:10.1109/TSP.2018.2802463)
36. Uhlich S. 2015 Bayes risk reduction of estimators using artificial observation noise. *IEEE Trans. Signal Process.* **63**, 5535–5545. (doi:10.1109/TSP.2015.2457394)
37. Duan F, Pan Y, Chapeau-Blondeau F, Abbott D. 2019 Noise benefits in combined nonlinear Bayesian estimators. *IEEE Trans. Signal Process.* **67**, 4611–4623. (doi:10.1109/TSP.2019.2931203)